International Journal of Nanomedicine

Dovepress
open access to scientific and medical research

Open Access Full Text Article

ORIGINAL RESEARCH

# Magnetic single-walled carbon nanotubes as efficient drug delivery nanocarriers in breast cancer murine model: noninvasive monitoring using diffusion-weighted magnetic resonance imaging as sensitive imaging biomarker



This article was published in the following Dove Press journal:
International Journal of Nanomedicine
23 December 2014
Number of times this article has been viewed

Achraf Al Faraj[1]
Abjal Pasha Shaik[2]
Asma Sultana Shaik[1,3]

[1]Department of Radiological Sciences, [2]Department of Clinical Lab Sciences, College of Applied Medical Sciences, [3]Prince Naif Health Research Center, College of Medicine, King Saud University, Riyadh, Saudi Arabia

**Purpose:** Targeting doxorubicin (DOX) by means of single-walled carbon nanotube (SWCNT) nanocarriers may help improve the clinical utility of this highly active therapeutic agent. Active targeting of SWCNTs using tumor-specific antibody and magnetic attraction by tagging the nanotubes with iron oxide nanoparticles can potentially reduce the unnecessary side effects and provide enhanced theranostics. In the current study, the in vitro and in vivo efficacy of DOX-loaded SWCNTs as theranostic nanoprobes was evaluated in a murine breast cancer model.

**Methods:** Iron-tagged SWCNTs conjugated with Endoglin/CD105 antibody with or without DOX were synthetized and extensively characterized. Their biocompatibility was assessed in vitro in luciferase (Luc2)-expressing 4T1 (4T1-Luc2) murine breast cancer cells using TiterTACS™ Colorimetric Apoptosis Detection Kit (apoptosis induction), poly (ADP-ribose) polymerase (marker for DNA damage), and thiobarbituric acid-reactive substances (oxidative stress generation) assays, and the efficacy of DOX-loaded SWCNTs was evaluated by measuring the radiance efficiency using bioluminescence imaging (BLI). Tumor progression and growth were monitored after 4T1-Luc2 cells inoculation using noninvasive BLI and magnetic resonance imaging (MRI) before and after subsequent injection of SWCNT complexes actively and magnetically targeted to tumor sites.

**Results:** Significant increases in apoptosis, DNA damage, and oxidative stress were induced by DOX-loaded SWCNTs. In addition, a tremendous decrease in bioluminescence was observed in a dose- and time-dependent manner. Noninvasive BLI and MRI revealed successful tumor growth and subsequent attenuation along with metastasis inhibition following DOX-loaded SWCNTs injection. Magnetic tagging of SWCNTs was found to produce significant discrepancies in apparent diffusion coefficient values providing a higher contrast to detect treatment-induced variations as noninvasive imaging biomarker. In addition, it allowed their sensitive noninvasive diagnosis using susceptibility-weighted MRI and their magnetic targeting using an externally applied magnet.

**Conclusion:** Enhanced therapeutic efficacy of DOX delivered through antibody-conjugated magnetic SWCNTs was achieved. Further, the superiority of apparent diffusion coefficient measurements using diffusion-weighted MRI was found to be a sensitive imaging biomarker for assessment of treatment-induced changes.

**Keywords:** carbon nanotubes, drug delivery systems, magnetic resonance imaging, diffusion-weighted MRI, breast cancer, nanomedicine

Correspondence: Achraf Al Faraj
Molecular and Cellular Imaging Lab, Department of Radiological Sciences, College of Applied Medical Sciences, King Saud University, Riyadh 11433, Saudi Arabia
Tel +966 11 46 96017/99664
Fax +966 11 46 93565
Email aalfaraj@ksu.edu.sa

submit your manuscript | www.dovepress.com
Dovepress
http://dx.doi.org/10.2147/IJN.S75074

## Introduction

Breast cancer remains one of the world's most devastating health problems and life-threatening diseases, especially among women. The adoption of periodic screening and the applications of current cancer treatments including surgical intervention, radiation, and chemotherapeutic drugs have considerably reduced the mortality of breast cancer patients. However, the side effects of chemotherapy pose a long-term challenge to patients' health, and most anticancer drugs have several drawbacks, including limited solubility and a poor nonselective biodistribution, thus resulting in severe damage to healthy tissues.[1,2] Therefore, novel theranostic tools that can specifically target tumor cells without affecting healthy cells and allow sensitive cancer detection in its early stage must be developed.[3]

From the various nanoscale drug delivery systems being investigated,[4] carbon nanotubes (CNTs), considered one of the most striking discoveries,[5] have been reported to be advantageous for cancer therapy and diagnosis.[6–8] Single-walled CNTs (SWCNTs) are one-dimensional nanomaterials envisaged as a single graphene sheet rolled into a seamless cylinder and having a diameter of 1–2 nm and a length ranging from as short as 50 nm up to few hundreds of micrometers and therefore can behave distinctly from spherical nanomaterials in biological environments. They combine several intriguing properties that make them attractive drug delivery nanocarriers.[9] First, through the enhanced permeability and retention effect,[10] SWCNTs exhibit higher accumulation in tumor tissues and therefore preferential delivery of therapeutic agents. Second, their needle-like shape facilitates transmembrane penetration and intracellular drug accumulation that is independent of additional functionalization and cell type[11] and can equally enter the cells via energy-dependent endocytic pathways.[12] Third, the high aspect ratio and surface areas of SWCNTs allow exceptional ability to encapsulate high therapeutic and diagnostic agents onto their surface or within their interior core via both covalent and noncovalent interactions.[13]

Doxorubicin (DOX), a member of the anthracycline class of chemotherapeutic agents commonly used for the treatment of several human cancers, is highly toxic and can result in severe suppression of hematopoiesis and gastrointestinal or cardiac toxicity.[14] Therefore, targeting of DOX by means of SWCNTs may help reduce the toxicity and improve the clinical utility of this highly active therapeutic agent. In addition, active targeting of SWCNTs using tumor-specific antibody and magnetic attraction by tagging the nanotubes with iron oxide nanoparticles can have the potential to reduce the unnecessary side effects associated with ineffective therapy and also provide early and better theranostics.[15]

To allow noninvasive sensitive tracking of SWCNTs after in vivo administration, different imaging modalities that rely on intrinsic characteristics of CNTs (ie, Raman scattering, high optical absorbance, near infrared [NIR] photoluminescence, photoacoustic and echogenic properties) or CNTs externally labeled with radionuclides (ie, positron emission tomography [PET]/single-photon emission computed tomography [SPECT] imaging) or gadolinium-based contrast agents (ie, magnetic resonance imaging [MRI]) have been validated.[15,16] Similarly, labeling SWCNTs with iron oxide nanoparticles was proposed to allow their sensitive detection using MRI in addition to offering the possibility of their magnetic targeting using external magnet to the primary tumor site. MRI has the superiority of simultaneously offering both anatomical (ie, using standard spin-echo sequence) and early quantitative assessments of disease responses (ie, using diffusion-weighted MRI [DW-MRI]) by characterizing the treatment-induced changes in tumor cell density.[17]

Water-stable and homogeneously dispersed polyvinylpyrrolidone (PVP)-functionalized short SWCNTs that were further tagged with iron nanoparticles and conjugated with Endoglin/CD105 monoclonal antibody for specific targeting to tumor sites, were recently developed.[15] Coupling antibody-active targeting with magnetic targeting by applying an external high-energy flexible magnet was found to improve the delivery of the magnetic SWCNTs to the tumor site in a murine breast cancer model. The purpose of this study was to validate the in vitro and in vivo efficacy of DOX-loaded SWCNTs as theranostic nanoprobes for breast cancer, endowed with improved ability to specifically target the tumor sites. Tumor progression and growth were monitored using noninvasive bioluminescence imaging (BLI) and MRI. SWCNTs biodistribution after intravenous injection was tracked using susceptibility-weighted MRI, and the benefit of DW-MRI as a sensitive imaging biomarker providing earlier and better assessment of disease response, was investigated.

## Materials and methods

### SWCNTs design and drug conjugation

Magnetic CD105-conjugated SWCNTs were prepared as previously described.[15] Briefly, ultrapure SWCNTs (Nanoshel LLC, Wilmington, DE, USA) were oxidized and shortened using ultra-sonication to generate 200–300 nm oxidized SWCNTs (oxSWCNTs). OxSWCNTs were conjugated with PVP polymer to obtain homogeneous and stable dispersion in water by employing short sonication treatment before final use. They were then suspended in distilled water containing $FeCl_2$ and $FeCl_3$ at 50°C under a nitrogen atmosphere, and

ammonium hydroxide solution was slowly added under continuous stirring to promote growth of the iron oxide nanoparticle crystals to obtain magnetic SWCNTs. For specific active targeting to tumor sites, magnetic SWCNTs were finally conjugated with a mouse Endoglin/CD105 monoclonal antibody (R&D Systems, Minneapolis, MN, USA) using 1-Ethyl-3-[3-dimethylaminopropyl]carbodiimide (EDC)/N-hydroxysulfosuccinimide (NHS) active ester method, and the binding of antibodies was monitored by recording the absorbance for proteins/antibodies at 280 nm and confirmed using in situ enzyme-linked immunosorbent assay (ELISA)-based assay.

To assess the efficiency of SWCNTs as drug delivery nanocarriers to tumor sites, magnetic CD105-conjugated SWCNTs were loaded with DOX antitumor drug (R&D Systems). DOX binding was performed by physicochemical interactions with the SWCNT surfaces at the different production steps by dispersing 150 µL of 5 mg/mL SWCNTs in 15 mL of 20 mM sodium phosphate buffer (pH 9.0) and 3 mL of 5 mM DOX hydrochloride (Millipore, Billerica, MA, USA). The mixture was sonicated in a water bath for 15 minutes and incubated overnight while stirring. Unbound DOX was removed by filtering using Millipore Amicon Ultra 30 kDa centrifugal filters. DOX loading was quantified using ultraviolet-visible spectroscopy at 490 nm based on a standard curve of DOX plotted using different concentrations of the drug in phosphate-buffered saline solution, to determine the exact amount of the loaded drug in the SWCNTs, as previously described.[18] The absorbance at 490 nm was recorded after the end of binding time both from control and from the supernatants of the conjugates.

## SWCNTs characterization

SWCNT complexes were characterized using transmission electron microscopy (TEM), UV–vis spectrophotometer, dynamic light scattering (DLS) zeta potential analysis, and electron spin resonance (ESR) spectroscopy. Their iron content was quantified using inductively coupled plasma mass spectrometry (ICP-MS), and their $r1$ and $r2^*$ magnetic resonance (MR) relaxivities were measured on a 4.7 T magnet.

Briefly, SWCNT samples were imaged using a Hitachi H7500 TEM system (Hitachi High-Technologies Corporation, Tokyo, Japan) operating at 100 kV and equipped with a Gatan BioScan (Gatan, Inc., Pleasanton, CA, USA) CCD camera to characterize their size and confirm their different conjugation steps.

UV–vis analyses were performed using a Cary 5000 UV–vis–NIR spectrophotometer (Agilent Technologies, Santa Clara, CA, USA), and the absorbance spectra (optical density) of SWCNT conjugates were measured at 490 nm to quantify the drug loading.

The zeta potential based on DLS was then measured in ultrapure water at 25°C using a Zetasizer Nano ZS90 (Malvern Instruments, Malvern, UK) to determine the electrical surface charge of SWCNT samples. Results were expressed as zeta potential (mV) ± standard deviation on an average of three measurements.

SWCNT samples were then analyzed using ESR to assess the quality of the CNT samples and check their magnetization effect. Spectra were recorded using a microESR system (Active Spectrum Inc., Foster City, CA, USA) operating in X band (9.6 GHz) at 2,000–4,000 G magnetic field range at room temperature.

SWCNTs iron loading and other metallic impurities were quantified using an Aurora M90 ICP-MS system (Bruker, Fremont, CA, USA). For ICP-MS quantification, SWCNT samples were mineralized with 2 mL of nitric acid in a microwave digestion system (Mars 6; CEM, Matthews, NC, USA).

Finally, the longitudinal ($r1$) and transverse ($r2^*$) relaxivities of SWCNT samples were then measured at 25°C as previously described[19] using a 4.7 T Pharmascan 47/16 Bruker magnet interfaced to ParaVision 5.1 software (Bruker Biospin GmbH, Rheinstetten, Germany).

## Tumor cell culture

Luciferase (Luc2)-expressing 4T1 (4T1-Luc2) murine breast cancer cells (PerkinElmer Inc., Waltham, MA, USA) that serve as an in vivo optical indicator of tumorigenesis to noninvasively track the tumor growth, were used in this study. 4T1 cells-induced breast cancer model was preferred in this study as its tumor growth and metastatic spread in Balb/c mice closely mimic a stage IV human breast cancer.[20] Cells were cultured in complete Roswell Park Memorial Institute 1640 medium containing 10% gamma-irradiated fetal bovine serum and 100 units/mL penicillin–streptomycin (Gibco, Life Technologies, Carlsbad, CA, USA) at 37°C in a humidified atmosphere containing 5% $CO_2$.

## SWCNTs in vitro biocompatibility

The biocompatibility of iron-tagged SWCNT (SWCNT·) vs CD105-conjugated DOX-loaded SWCNT· (SWCNT· + CD105 + DOX) samples was assessed in vitro in 4T1 cells. Experiments were conducted to assess the ability of SWCNT complexes to induce apoptosis (TiterTACS™ Colorimetric Apoptosis Detection Kit [TACS; R&D Systems] assay),

the activation of poly (ADP-ribose) polymerase (PARP) as a marker for DNA damage (PARP assay), and generation of thiobarbituric acid-reactive substances (TBARS) due to oxidative stress (TBARS assay). Cells were incubated in triplicates ($10^4$ cells/well) with different concentrations (2.5 µg/mL, 5 µg/mL, 7.5 µg/mL, and 10 µg/mL) of SWCNT· or SWCNT· + CD105 + DOX conjugates for 2 hours, 24 hours, 48 hours, and 72 hours, and the results were compared to untreated cells.

### TACS assay

The TACS (R&D Systems) was used to detect apoptosis using TACS-Sapphire™ technology as per the manufacturer's instructions. After incubation with the different SWCNT samples, the cells were washed, treated with proteinase K, and labeled with a buffer containing a nucleotide mix and TdT enzyme. The cells were then treated with streptavidin–horseradish peroxidase (HRP) and stained with TACS sapphire beads. The absorbance of the samples was measured at 450 nm using an ELISA plate reader (BioTek, Winooski, VT, USA).

### PARP assay

DNA damage caused by the SWCNT complexes at various concentrations and time intervals was assessed by estimating the PARP using PARP assay kit (R&D Systems). Following incubation with the SWCNT samples, the cells were lysed using a cell lysis buffer, and the cell lysates were transferred into histone-coated plates. A ribosylation reaction was then performed, and the reactions were detected using the streptavidin–HRP and substrate. After stopping the reactions using a stop solution, the plates were read at 450 nm using the BioTek ELISA plate reader.

### TBARS assay

TBARS parameter assay kit (R&D Systems) was used to measure the overall oxidative stress caused by either SWCNT· or SWCNT· + CD105 + DOX at different concentrations and time intervals in 4T1 cells as per the manufacturer's instructions. Briefly, the cultured 4T1 cells were equilibrated overnight, treated with SWCNT samples, and then washed and lysed using a cell lysis buffer. Plates were incubated with an acid reagent for 15 minutes, centrifuged, and supernatants were treated with thiobarbituric acid reagent for 2–3 hours at 45°C–50°C. The absorbance of the samples was measured at 532 nm using the BioTek ELISA plate reader.

## SWCNTs in vitro therapeutic efficacy

The in vitro efficacy of DOX-loaded SWCNTs was assessed by BLI using an IVIS Lumina Series III preclinical imaging system (PerkinElmer Inc.). SWCNT·, SWCNT· + DOX, and SWCNT· + CD105 + DOX suspensions were incubated with 4T1-Luc2 cells ($2\times10^4$ cells/well) in 24-well plates for 2 hours, 24 hours, and 48 hours, and compared with free DOX suspensions and untreated cells. DOX concentration was calculated based on the loaded drug in the SWCNT samples. BLI of the cells was performed after 10-minute incubation with 150 µg/mL d-Luciferin (1×) according to the manufacturer's specifications (PerkinElmer Inc.). Photon flux was measured at the different investigation time points using Living Image software (version 2.5) and presented as radiance efficiency (ρ/s/cm$^2$/sr). Bioluminescence values were then represented as percent photon flux of untreated or control values.

## Animal preparation and study design

Female Balb/c mice (aged 6 weeks) were obtained from the University's main animal care center. All animal procedures were performed in accordance with the national guidelines for the care of laboratory animals, and the study was approved by the Ethical Committee of the College of Applied Medical Sciences (agreement number: CAMS07/3334). During the different imaging protocols, each animal was anesthetized with 1.5%–2% Sevoflurane anesthesia.

A tumor model was established by injecting $10^6$ 4T1-Luc2 cancerous cells in the left inguinal mammary fat pad of Balb/c mice. The injection site was shaved using a depilatory cream for easier administration of tumor cells and for better contact of the magnet over the tumor site.

In order to assess the in vivo efficacy of DOX-loaded SWCNTs, tumor-bearing mice were divided into six groups (n=6) and received two 100 µL intravenous injections, with 1-week interval time, of the following suspensions: control (ie, physiological serum); DOX (ie, 100 µg per mice, corresponding to 5 mg/kg); SWCNT + CD105, SWCNT· + CD105, SWCNT + CD105 + DOX, and SWCNT· + CD105 + DOX (ie, 50 µg CD105-conjugated SWCNT with or without either iron nanoparticles (·) or DOX drug). A high-energy flexible magnet was maintained over the tumor site during 2 hours postinjection using a 3M™ Transpore™ medical tape (3M, St Paul, MN, USA). The magnetic properties and polarity were previously optimized to allow enhanced magnetic targeting of iron-tagged SWCNTs toward the primary tumor site.[15]

## Noninvasive bioluminescence tumor imaging

Noninvasive BLI was performed on tumor-bearing mice to monitor the tumor progression and eventual metastasis after 4T1-Luc2 tumor cells inoculation and to assess the therapeutic effect of DOX-loaded SWCNT complexes before

and at 3 days, 7 days, 10 days, and 14 days after the second injection of SWCNTs and DOX suspensions (Figure 1). Mice were intraperitoneally (ip) injected 10 minutes before imaging with the d-Luciferin (150 mg Luciferin/kg body weight) according to the manufacturer's protocol, and the radiance efficiency was assessed during the follow-up investigation in the primary tumor site.

## Noninvasive MRI

### MR monitoring of tumor site

Tumor volume was quantified during the follow-up investigation study (Figure 1), before and after DOX or SWCNT complexes injection, using a fast spin echo Turbo rapid acquisition with refocused echoes (RARE) sequence with Time of repetition (TR)/Time of echo (TE) =2,500/10 ms, RARE factor =8, four averages, and 100 µm ×100 µm in-plane resolution. Continuous 1 mm thick slices were used to cover the entire tumor region.

### MR-sensitive detection of SWCNTs

In order to detect the homing of SWCNTs to the main tumor site after their intravenous injection, susceptibility-weighted multi-gradient echo sequence with TR =300 ms, and increasing TEs starting from 5 ms with 15 echoes of 5 ms echo spacing, four averages, flip angle =30°, and 100 µm ×100 µm in-plane resolution, was performed. *T2** maps were generated using ImageJ software (NIH, Bethesda, MD, USA).

### Diffusion-weighted MRI

Apparent diffusion coefficient (ADC) measurements were also performed directly after *T2** quantifications as a sensitive imaging biomarker providing early and better assessment of disease treatment. Data were acquired using a standard pulsed spin echo sequence with three *b* values (0 s/mm$^2$, 500 s/mm$^2$, and 1,000 s/mm$^2$), and the gradients were simultaneously applied along the three orthogonal directions ($x$, $y$, and $z$). Scan acquisition parameters were as follows: TR/TE =2,500/30 ms, bandwidth =50 kHz, gradient duration $\delta$=3 ms, gradient interval $\Delta$=20 ms, and 200 µm ×200 µm in-plane resolution. A total of three to five 1 mm thick slices were used to cover the tumor sites. To construct an ADC parametric map, signal intensities from DW images acquired at the three *b* values were fit for each image voxel using ImageJ software using the Stejskal–Tanner equation: $S(b) = S_0 \times e^{-b \times ADC}$, where $S_0$ and $S(b)$ are the signal intensities before and after application of diffusion gradients, respectively. Regions of interest were drawn on the *b*=0 s/mm$^2$ DW image within tumor site, at the slice in which the largest ROI could be drawn.

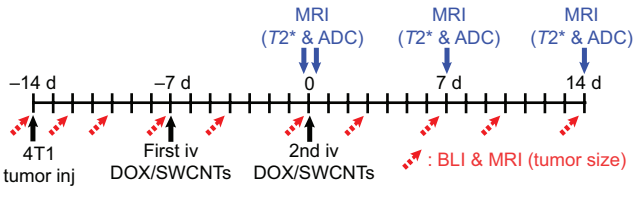


**Figure 1** Study design indicating the timing of 4T1 tumor cells injection in the left inguinal mammary fat pad, the first and second iv injection of DOX or the different SWCNT conjugates, and the different BLI and MRI protocols.

**Abbreviations:** DOX, doxorubicin; SWCNT, single-walled carbon nanotube; BLI, bioluminescence imaging; MRI, magnetic resonance imaging; inj, injection; ADC, apparent diffusion coefficient; d, days; iv, intravenous.

## Statistical analysis

Data presented as mean values ± standard deviation were analyzed by Student's *t*-test using SPSS v12.0 (SPSS Inc., Chicago, IL, USA) software. A *P*-value <0.05 was considered significant for all tests.

# Results

## SWCNTs design, drug loading, and characterization

Iron-tagged SWCNTs functionalized with PVP polymer and conjugated with mouse Endoglin/CD105 monoclonal antibodies were successfully obtained. They have an average tube length of 200–300 nm quantified on several TEM images (Figure 2A). TEM also allowed the detection of a thin and transparent layer of low contrast around the CNTs surface confirming the binding of PVP (dotted arrows). Chemically attached and adsorbed iron oxide nanoparticles with approximately 4–5 nm size (solid arrows) were observed on SWCNT samples using TEM, which revealed that numerous free areas were available on SWCNTs surface for further conjugation with either antibodies or drugs. UV–vis spectroscopy analysis (Figure 2B) confirmed the binding of PVP polymer by the presence of the characteristic peak at 235/256 nm and the conjugation of Endoglin/CD105 antibodies by monitoring the absorbance for proteins/antibodies at 280 nm. UV–vis spectroscopy at 490 nm equally allowed quantification of DOX loading based on a standard curve of DOX plotted using different concentrations of the drug in phosphate-buffered saline solution to determine the exact amount of the loaded drug in the SWCNTs. The absorbance at 490 nm ($OD_{490\ nm}$) was shown to increase from 0.731 to 0.805 after DOX conjugation, and the drug loading in the CNT samples was estimated to 2 mg of DOX per 1 mg of SWCNTs, corresponding to a loading of 200%.

Zeta potential analyses (Figure 2C) performed to further characterize SWCNT samples revealed a highly negative surface charge (–25.2±1.1 mV) for oxSWCNTs. After PVP binding and iron oxide tagging, zeta potential of SWCNTs

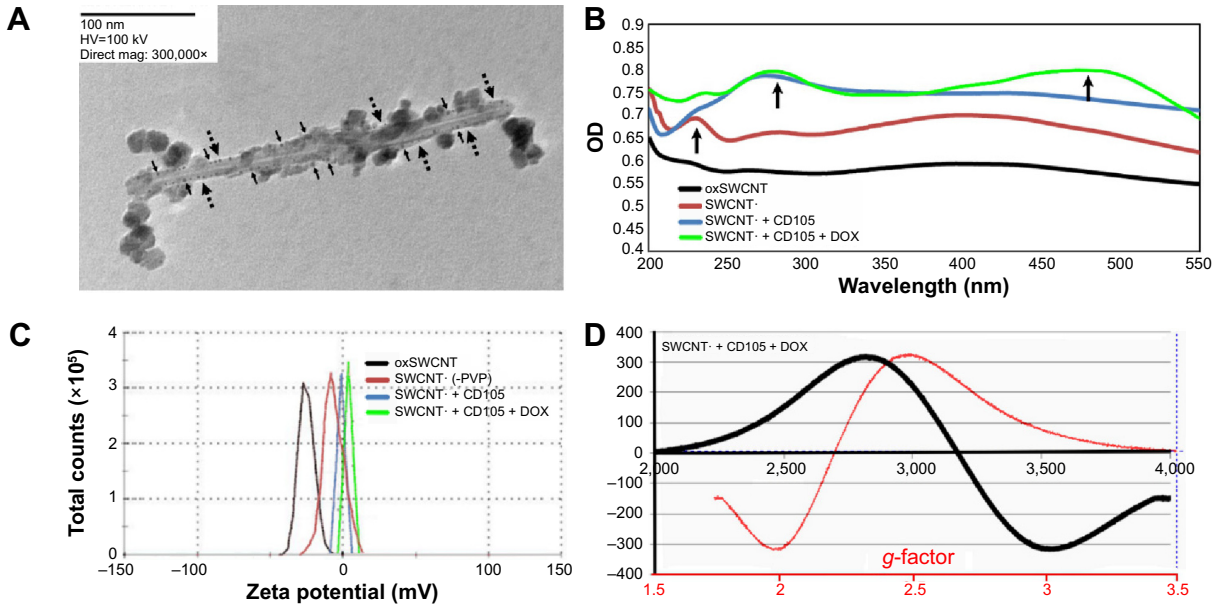


**Figure 2** SWCNTs characterization.

**Notes:** (**A**) Representative TEM image of iron-tagged, CD105-conjugated, and DOX-loaded SWCNTs (SWCNT· + CD105 + DOX). TEM also allowed the detection of a thin and transparent layer of low contrast around the CNTs surface confirming the binding of PVP (dotted arrows). Chemically attached and adsorbed iron oxide nanoparticles with approximately 4–5 nm size (solid arrows) were observed on SWCNT samples using TEM, which revealed that numerous free areas were available on SWCNTs surface for further conjugation with either antibodies or drugs. (**B**) UV–vis spectra of oxSWCNT, SWCNT·, SWCNT· + CD105, and SWCNT· + CD105 + DOX revealing characteristic peaks at 235/256 nm for PVP polymer functionalization, at 280 nm for CD105 antibodies conjugation, and at 490 nm for DOX drugs loading. (**C**) Dynamic light scattering zeta potential spectra of oxSWCNT, SWCNT· before PVP functionalization, SWCNT· + CD105, and SWCNT· + CD105 + DOX showing the corresponding surface charge at the different steps of carbon nanotubes synthesis. (**D**) Characteristic ESR spectrum of SWCNT· + CD105 + DOX sample recorded at room temperature using a magnetic field ranging from 2,000 Gauss to 4,000 Gauss.

**Abbreviations:** TEM, transmission electron microscopy; DOX, doxorubicin; SWCNT, single-walled carbon nanotube; oxSWCNT, oxidized SWCNT; PVP, polyvinylpyrrolidone; ESR, electron spin resonance; OD, optical density; Mag, magnification; UV-vis, ultraviolet-visible.

was found to progressively increase to −6.66±0.8 mV and −1.49±0.6 mV, respectively, to become slightly positive (ie, 0.499±0.5 mV and 0.751±0.5 mV) after either CD105 antibodies or DOX conjugations.

Furthermore, ESR spectroscopy analyses performed to characterize the iron-tagged SWCNT + CD105 + DOX samples revealed a typical ESR spectrum (Figure 2D), which consisted of three resonance lines: a wide resonance line with a *g*-factor higher than 2.1 assigned to magnetic iron oxide nanoparticles, a broad line localized near the free-electron *g*-value and assigned to conducting electrons delocalized over the conducting domains of CNTs (ie, in interaction with the electronic spins assigned to magnetic impurities), and a narrow line, superimposed on the broad one, assigned to paramagnetic impurities located on the CNTs.

Quantification of iron load and other metallic impurities in the SWCNT samples using ICP-MS revealed a 40% iron oxide nanoparticles load (w/w) on the CNTs and confirmed the high purity of SWCNT samples from other metal impurities.

Finally, measurements of $r1$ and $r2^*$ transverse relaxivities at 4.7 T MRI magnet exhibited very high MR $r2^*$ relaxivities values for iron-tagged SWCNT samples (ie, 231.331±8.44 $mM^{-1}$ $s^{-1}$, 213.546±7.78 $mM^{-1}$ $s^{-1}$, and 210.183±9.24 $mM^{-1}$ $s^{-1}$ for SWCNT·, SWCNT· + CD105, and SWCNT· + CD105 + DOX samples, respectively) compared to 21.399±8.39 $mM^{-1}$ $s^{-1}$ for ultrapure SWCNT samples before iron loading. For both samples, $r1$ values were found negligible with 0.0913±0.0122 $mM^{-1}$ $s^{-1}$.

## DOX-conjugated SWCNTs in vitro biocompatibility and therapeutic efficacy

TACS, PARP, and TBARS assays showed that SWCNT· + CD105 + DOX conjugates were capable of increasing apoptosis, DNA damage, and oxidative stress in 4T1 cells in a time- and dose-dependent manner. A dramatic increase in apoptosis was noted as early as 24 hours with CD105-conjugated SWCNT· + DOX (Figure 3A). A considerable increase in DNA damage was noted with SWCNT· + CD105 + DOX compared to non-conjugated SWCNT· ($P<0.05$) (Figure 3B). Comparable increases were seen in oxidative stress in both SWCNT· and SWCNT· + CD105 + DOX-treated cells (Figure 3C).

BLI of breast cancer murine 4T1-Luc2 cells, which was performed to assess the efficacy of DOX drugs loaded in SWCNTs and compare with free drugs, revealed a decrease

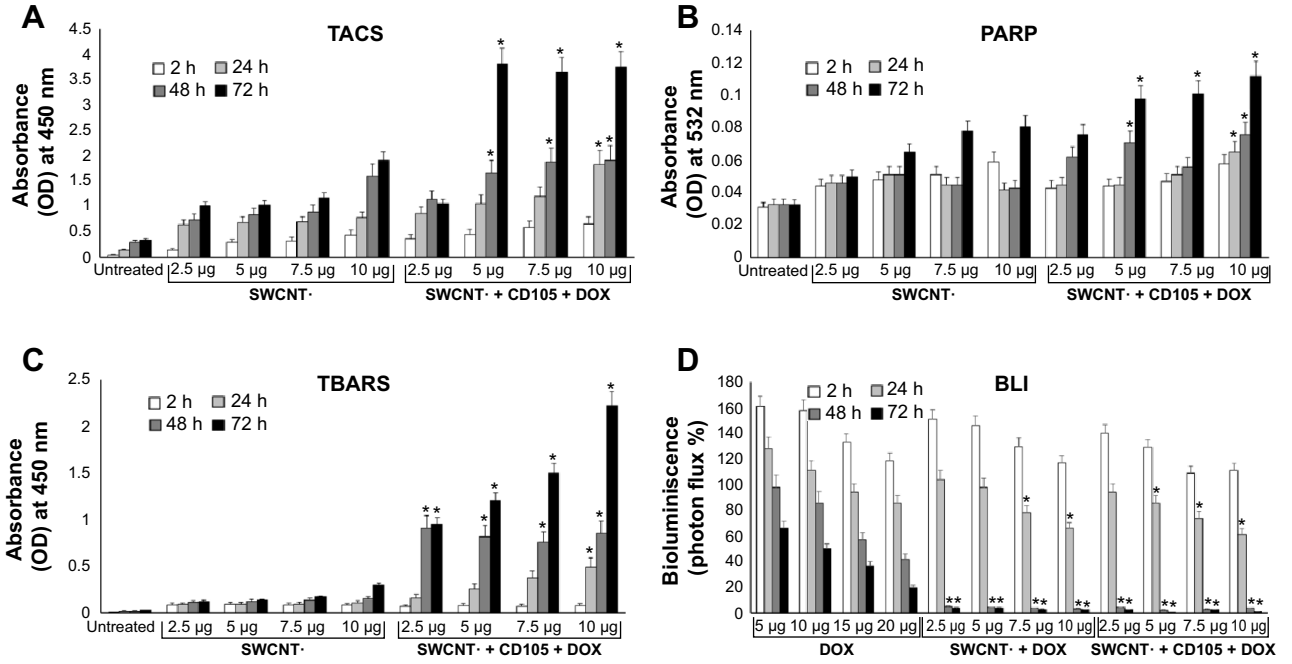


**Figure 3** SWCNTs biocompatibility assessments.

**Notes:** (**A**) cell apoptosis (TACS), (**B**) DNA damage (PARP), and (**C**) oxidative stress generation (TBARS) of iron-tagged SWCNTs (ie, SWCNT·) and CD105 and DOX-conjugated SWCNT· (ie, SWCNT· + CD105 + DOX) incubated with 4T1 tumor cells. *$P<0.05$ vs SWCNT·. Therapeutic efficacy (**D**) (percentage of photon flux by bioluminescence imaging) of free DOX drugs compared to DOX-loaded SWCNT· (ie, SWCNT· + DOX and SWCNT· + CD105 + DOX) conjugates. Cells were incubated for 2 hours, 24 hours, 48 hours, or 72 hours with either SWCNT samples at 2.5 µg/mL, 5 µg/mL, 7.5 µg/mL, or 10 µg/mL or DOX suspensions at corresponding drug loading at 5 µg/mL, 10 µg/mL, 15 µg/mL, and 20 µg/mL. *$P<0.05$ vs DOX. Data expressed as mean ± SD, n=3 per group.

**Abbreviations:** TACS, TiterTACS™ Colorimetric Apoptosis Detection Kit; PARP, poly (ADP-ribose) polymerase; TBARS, thiobarbituric acid-reactive substances; SWCNT, single-walled carbon nanotube; DOX, doxorubicin; SD, standard deviation; OD, optical density; BLI, bioluminescence imaging; h, hours.

in photon flux or radiance efficiency in a time- and dose-dependent manner at various concentrations of DOX, SWCNT· + DOX, and SWCNT· + CD105 + DOX suspensions (Figure 3D). A substantial decrease in bioluminescence indicated the efficacy of DOX. In addition, SWCNT· + DOX and SWCNT· + CD105 + DOX were capable of inducing cell death at a higher frequency compared to free DOX. Bioluminescence was drastically lower after 48 hours of exposure and more prominent in the SWCNT· + CD105 + DOX group ($P<0.05$).

## Noninvasive BLI and MRI

Noninvasive BLI performed on tumor-bearing mice revealed the successful tumor growth in the primary injection site in the left inguinal mammary fat pad (Figure 4A). Following injection of SWCNT + CD105 and SWCNT· + CD105 samples, the radiance efficiency was found to gradually increase and become more prominent with the progression of metastasis in the upper thoracic region (ie, the lung) observed 3 weeks post-tumor cells injection (ie, 7 days post-SWCNTs injection). Following injection of free DOX drug, an attenuation of bioluminescence was measured, and a less prominent progression of metastasis was noticed. Interestingly, following injection of drug-conjugated SWCNT + DOX and to a higher extent in iron-tagged samples (ie, SWCNT· + CD105 + DOX) magnetically targeted to the primary tumor site, radiance efficiency was found to considerably decrease along with inhibition of metastasis (Figure 4B).

Quantification of primary tumor growth assessed using MRI (Figure 5) revealed a progressive increase in tumor volume in DOX, SWCNT + CD105, and SWCNT· + CD105 groups during the 1-month follow-up investigation study. However, in SWCNT + CD105 + DOX and to a higher extent in SWCNT· + CD105 + DOX groups, tumor size progressively decreased after drug-loaded CNTs intravenous injection.

*T*2* quantifications performed at 0 hours (preinjection), 2 hours, 7 days, and 14 days after the second intravenous injection of free drugs or SWCNTs conjugated samples revealed a significant attenuation for both iron-tagged SWCNT samples (Figure 6A). Quantitatively, *T*2* values were found equal to 8.9±1.1 ms and 9.2±1.9 ms at 2-hour investigation time point for SWCNT· + CD105 and SWCNT· + CD105 + DOX, respectively, compared to 21.9±1.2 ms and 23.1±1.3 ms at preinjection time point. *T*2* attenuations were found to slightly decrease in a time-dependent manner; however,

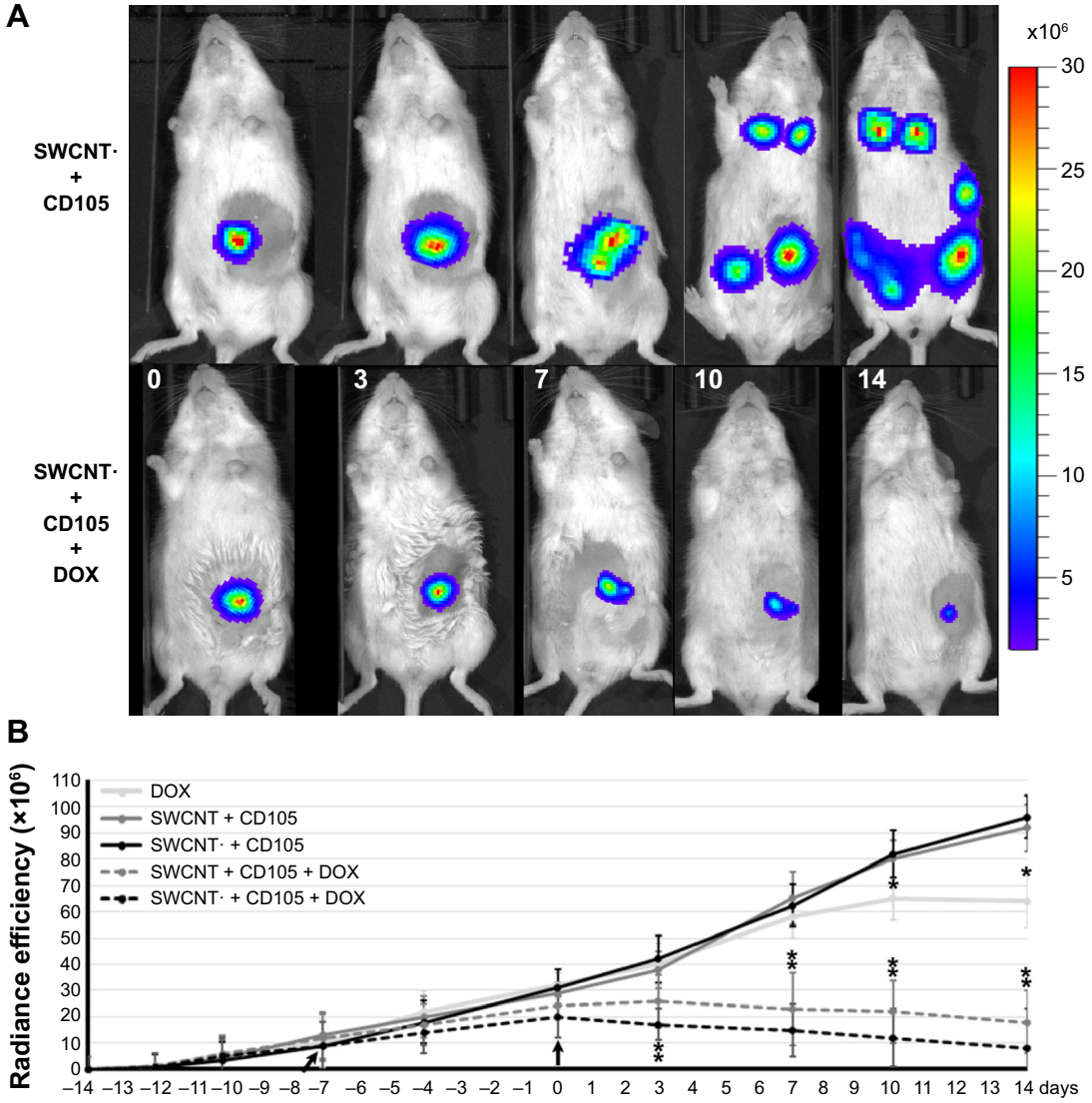


**Figure 4** Noninvasive bioluminescence imaging (BLI).

**Notes:** (**A**) Representative noninvasive bioluminescence images (radiance efficiency) of tumor-bearing mice at 0 days, 3 days, 7 days, 10 days, and 14 days following injection of either SWCNT· + CD105 (upper row) or DOX-loaded SWCNT· + CD105 (lower row) showing the progression of tumor and eventual metastasis following inoculation of 4T1-Luc2 breast cancer cells in the left inguinal mammary fat pad. (**B**) Quantitative assessments of radiance efficiency following iv injection of either free DOX or CD105-conjugated SWCNT samples with or without either iron tagging (·) or drug loading (DOX) performed to assess treatment-induced responses. Black arrows highlight the time of DOX or SWCNT conjugate injections. Data expressed as mean ± SD, n=6 per group. *$P<0.05$ vs SWCNT + CD105.

**Abbreviations:** SWCNT, single-walled carbon nanotube; DOX, doxorubicin; Luc2, luciferase; SD, standard deviation; iv, intravenous.

they were still statistically lower than preinjected values at 2 weeks postinjection investigation time point ($P<0.05$) (Figure 6B).

On the other hand, ADC measurements quantified in the primary tumor injection site in the left inguinal mammary fat pad (Figure 7A) were found to increase slightly after intravenous injection of free drug suspensions at 7 days postinjection; however, this increase was not found to be statistically different ($P<0.05$) when compared to pre-DOX-injected ADC values. While no difference was observed in SWCNT + CD105 group, iron oxide nanoparticles, tagged to the antibodies-conjugated CNT samples and magnetically attracted by the external magnet placed over the tumor site, were found to induce a significant decrease in ADC values during the 2-week investigation. An ADC value of $(0.619\pm0.061)\times10^{-3}$ mm$^2$/s was measured at 2 hours postinjection compared to $(0.855\pm0.043)\times10^{-3}$ mm$^2$/s preinjection of SWCNT· + CD105 samples. Interestingly, a time-dependent significant increase in ADC was observed after SWCNT + DOX + CD105 injection. Conversely, after injection of the corresponding iron-tagged sample, a significant attenuation was observed at 2 hours with $(0.638\pm0.057)\times10^{-3}$ mm$^2$/s followed by a high increase in ADC with $(1.089\pm0.064)\times10^{-3}$ mm$^2$/s and

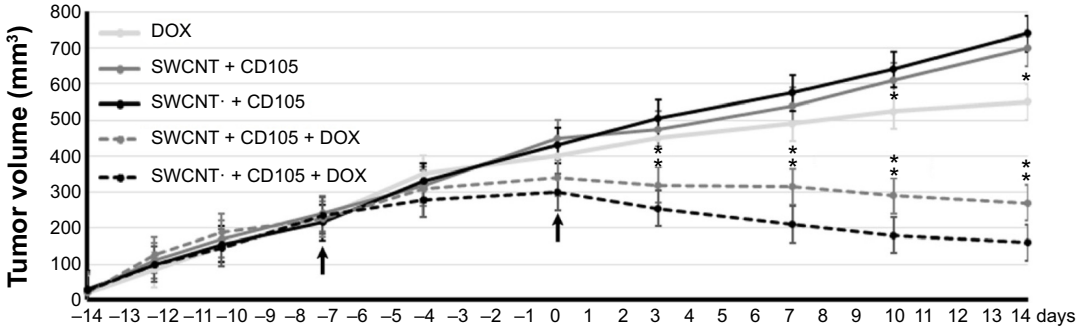


**Figure 5** Tumor volume quantification using MRI.
**Notes:** Tumor volume quantified by MRI using a fast spin echo Turbo RARE following injection of 4T1-Luc2 breast cancer cells in the left inguinal mammary fat pad of a murine model. Tumor volume was measured after iv injection of free DOX and CD105-conjugated SWCNT samples with or without either iron tagging (·) or drug loading (DOX) as theranostic nanoprobes. Black arrows highlight the time of DOX or SWCNT conjugate injections. Data expressed as mean ± SD, n=6 per group. *$P$<0.05 vs SWCNT + CD105.
**Abbreviations:** MRI, magnetic resonance imaging; RARE, rapid acquisition with refocused echoes; Luc2, luciferase; DOX, doxorubicin; SWCNT, single-walled carbon nanotube; SD, standard deviation; iv, intravenous.

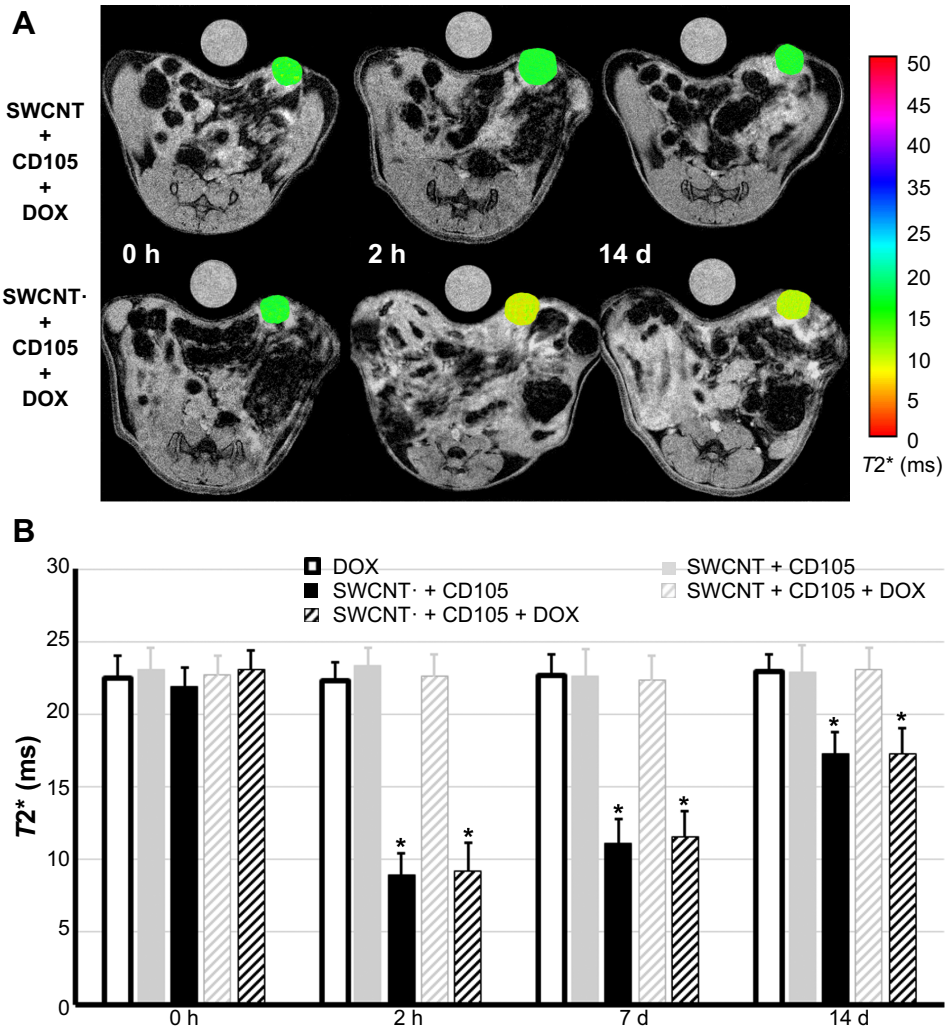


**Figure 6** T2* quantifications using MR imaging.
**Notes:** (**A**) Representative MR images of tumor-bearing mice at 0 hours (preinjection), 2 hours, and 14 days post-iv injection with CD105 antibody-conjugated, DOX-loaded SWCNTs conjugated with (·) or without iron oxide nanoparticles tagging, which were acquired using multi-gradient echo MR pulse sequence at 4.7 T magnet. Images with the shortest echo time (ie, TE =5 ms) were presented. *T2** values were quantified in the tumor sites and presented in the color map. (**B**) Quantification of *T2** (ms) in the primary tumor site at 0 hours (preinjection), 2 hours, 7 days, and 14 days post-iv injection with either free DOX suspensions or CD105-conjugated SWCNT nanocarriers with or without either iron-tagging (·) or drugs loading (DOX). Data expressed as mean ± SD, n=6 per group. *$P$<0.05.
**Abbreviations:** MR, magnetic resonance; DOX, doxorubicin; SWCNT, single-walled carbon nanotube; SD, standard deviation; h, hours; d, days; post-iv, post-intravenous.

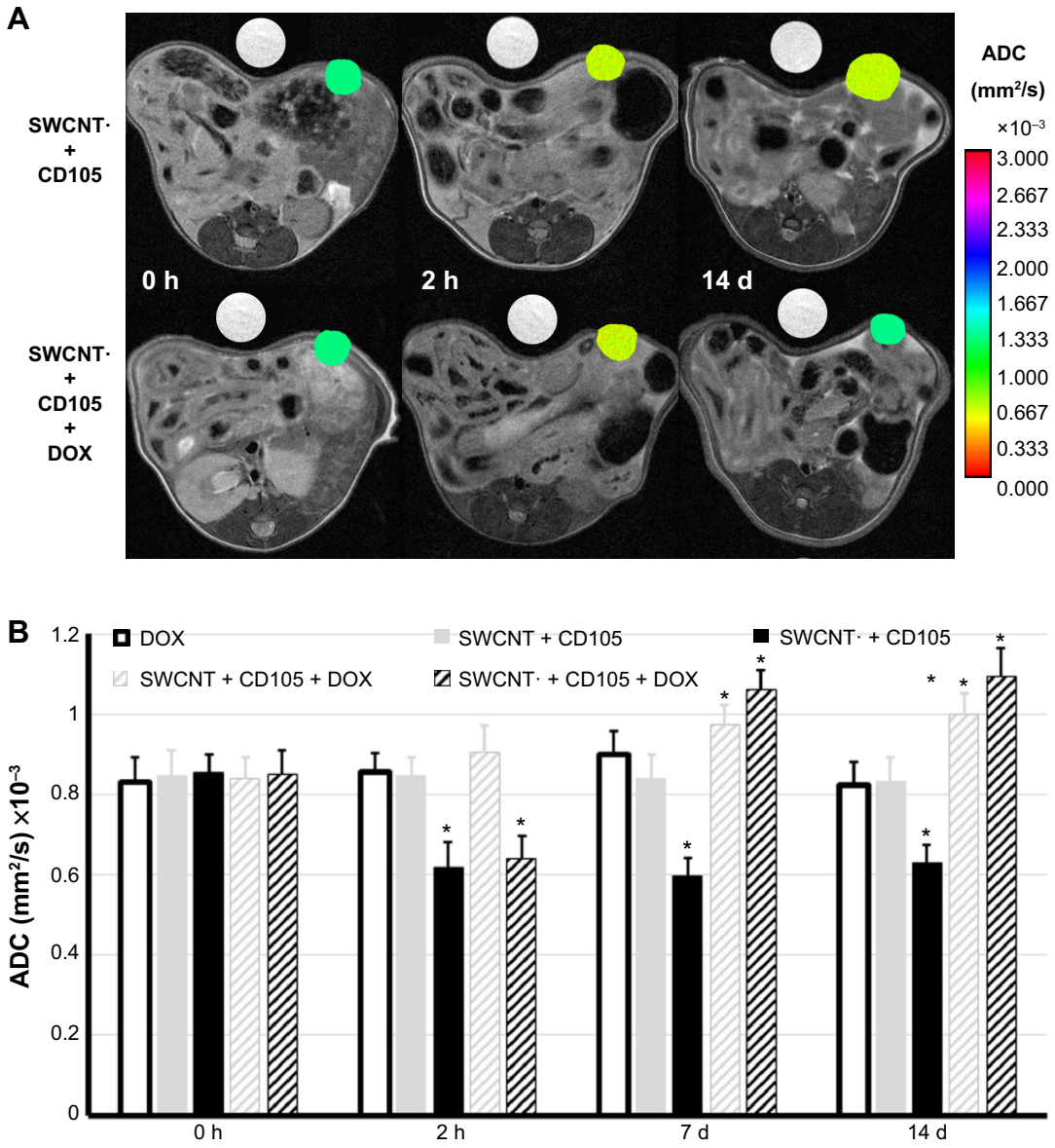


**Figure 7** ADC measurements using DW-MR imaging.

**Notes:** (**A**) Representative MR images of tumor-bearing mice at 0 hours (preinjection), 2 hours, and 14 days post-iv injection with iron-tagged, CD105-conjugated SWCNTs (ie, SWCNT· + CD105) before and after DOX loading (ie, SWCNT· + CD105 + DOX), which were acquired using fast spin echo MR pulse sequence at 4.7 T magnet. Images with the shortest *b* value (ie, *b*=0) were presented. ADC measurements in the tumor sites are presented as a color map. (**B**) Quantification of ADC values (mm²/s) in the primary tumor site at 0 hours (preinjection), 2 hours, 7 days, and 14 days post-iv injection with either free DOX suspensions or CD105-conjugated SWCNT nanocarriers with or without either iron-tagging (·) or drugs loading (DOX). Data expressed as mean ± SD, n=6 per group. *$P<0.05$.

**Abbreviations:** MR, magnetic resonance; SWCNT, single-walled carbon nanotube; DOX, doxorubicin; DW, diffusion-weighted; ADC, apparent diffusion coefficient; SD, standard deviation; h, hours; d, days; post-iv, post-intravenous.

(1.095±0.067)×10$^{-3}$ mm$^2$/s observed at 7 days and 14 days, respectively (Figure 7B).

## Discussion

Our recent studies have confirmed that the application of an external optimized magnet over a tumor site not only enhanced the active and selective targeting of PVP-functionalized, iron-tagged, and antibody-conjugated SWCNT nanocarriers but also has the potential advantage for their in vivo detection using noninvasive MRI.[15] In the current study, we investigated the therapeutic efficacy of these SWCNT conjugates to enhance the delivery of DOX to the primary tumor site in a murine breast cancer model. Furthermore, the superiority of ADC measurements in DW-MRI as a sensitive imaging biomarker to detect earlier and better treatment-induced changes, was assessed.

To validate our approach, DOX drugs were first successfully conjugated to the SWCNT nanocarriers. The DOX-conjugated SWCNTs were extensively assessed using TEM, UV–vis spectroscopy, DLS zeta potential, and

ESR spectroscopy to quantify their drug loading and characterize their morphology, surface charge, and magnetization effect. In addition, the iron loading was measured using ICP-MS, and their *r*1 and *r*2* relaxivities were evaluated using MRI. Liu et al reported that by simply mixing DOX with the SWCNTs, the drug could be adsorbed onto the sidewalls of SWCNTs via π–π stacking interactions.[21] By optimizing the initial DOX concentration (ie, 5 mM) and the solution pH (ie, pH 9), an efficient loading of 200% was obtained. This loading capacity was comparable to what has been reported in other studies,[18] which confirm that PVP polymer, the iron oxide nanoparticles, and the antibodies conjugated to the nanotubes did not interfere with the capacity of the nanotubes to further non-covalently attach DOX drugs. No variation in size and surface charge was observed after DOX loading compared to antibody-conjugated SWCNTs, and the tagged iron oxide nanoparticles were optimized to allow high magnetization effect for a better noninvasive detection using MRI as assessed by ESR and MR relaxivity measurements.

The cytotoxicity of PVP-functionalized SWCNT· particles has been previously established at various concentrations and time intervals.[15] In the current study, experiments were conducted to assess the in vitro therapeutic efficacy of DOX-conjugated SWCNTs after their incubation with 4T1 breast cancer cells for 2 hours, 24 hours, 48 hours, and 72 hours at different concentrations, and their ability to induce apoptosis, DNA damage, and oxidative stress. The SWCNT· + CD105 + DOX conjugates increased apoptosis, DNA damage, and oxidative stress in 4T1 cells in a time- and dose-dependent manner compared to SWCNT· alone. Further, BLI revealed a more prominent decrease in photon flux or radiance efficiency in a time- and dose-dependent manner for SWCNT· + CD105 + DOX compared to either SWCNT· + DOX or free DOX, which is likely due to the targeted release of DOX inside cell endosomes and lysosomes using the SWCNT nanocarriers. It has been shown that the CNTs, owing to their shape, can penetrate the cell membranes and enter the cellular components without causing cell damage.[22,23] It is worth pointing out that the conjugation of targeted antibodies (ie, Endoglin/CD105) to the CNT nanocarriers can enhance the tumor uptake by enhancing selectivity.[24] We have noted that CD105-conjugated CNTs ensured selective targeting of 4T1 tumor cell line in vitro.

Antibody-conjugated magnetic SWCNTs magnetically targeted to the primary tumor site using an optimized magnet and actively targeted to cancerous cells by Endoglin/CD105 antibodies conjugation were investigated in the current study as novel theranostic nanoprobes to enhance the delivery of DOX drug and offer greater selectivity after in vivo administration. Noninvasive BLI was implemented to monitor the tumor growth in mice during the first few days after 4T1-Luc2 breast cancer cells inoculation and to monitor the potential metastasis progression starting from 3 weeks post-tumor cells administration.[25] These noninvasive imaging protocols allowed real-time in vivo monitoring of tumor growth in mice.

The active targeting of DOX through SWCNT + CD105 nanoprobes and to a higher extent their active and magnetic targeting via SWCNT· + CD105 was found to considerably decrease the primary tumor site and may have inhibited the development of metastasis in the tumor-bearing mice lung. Quantification of tumor volume using MRI corroborated the noninvasive BLI readouts with a significant attenuation of tumor progression after injection of SWCNT + CD105 + DOX and to a higher extent SWCNT· + CD105 + DOX conjugates, while the tumor volume gradually increased in size after DOX suspensions administration or nondrugs-conjugated SWCNT nanoprobes. The tissue localization of SWCNT nanocarriers at the primary tumor site has been established histopathologically in our previous study[15] confirming the specific and enhanced targeting. While this positively indicates the potential applications of DOX-containing nanocarriers in controlling the spread of cancer, further experiments are needed to specifically determine the extent of metastasis delay, inhibition, and progression using antibody-conjugated and by magnetically targeting drug nanocarriers.

The decreases in *T*2* values also confirmed the enhanced magnetic targeting of iron-tagged SWCNT complexes to the tumor site driven by the magnet positioned over the primary tumor site. Iron oxide nanoparticles produced a high susceptibility or magnetization effect by disturbing the homogeneity of the magnetic field. *T*2* attenuation was found to progressively decrease in a time-dependent manner, most probably due to the degradation, using antibody-conjugated and magnetically-targeted drug nanocarriers.

Finally, ADC measurements in DW-MRI introduced as a sensitive imaging biomarker to detect treatment-induced changes were found to significantly increase in a time-dependent manner after the injection of DOX-conjugated SWCNT complexes. An increase in ADC was reported as a reproducible good index for efficient cancer therapy, which is directly related to the number of killed tumor cells and thought to be due to the liberation of water into the extracellular space as a result of cell necrosis.[17] Interestingly, the iron oxide nanoparticles presented in SWCNT· + CD105 + DOX samples, which were found to express an attenuation in *T*2* once reaching the tumor site, produced a transient decrease in ADC at 2 hours post-administration, due to the disturbance of

the magnetic field homogeneity. This transient decrease was followed by a high increase at 7-day and 14-day investigation time points as an index of treatment-induced changes. Therefore, magnetic tagging of SWCNTs was found to produce significant discrepancies in ADC values providing a higher contrast to detect treatment-induced variations as noninvasive imaging biomarker. In addition, it allowed their sensitive noninvasive diagnosis using susceptibility-weighted MRI and their magnetic targeting using an externally applied optimized magnet.

## Conclusion

The current study showed that DOX delivered through antibody-conjugated magnetic SWCNTs improved the in vitro and in vivo efficacy of DOX-loaded SWCNTs in addition to providing an improved ability to specifically target the tumor sites. Our results indicate that drugs delivered through this mechanism may not only have potential to reduce tumor size but could also prevent progression to metastasis. In addition, the superiority of ADC measurements using DW-MRI was established as a sensitive imaging biomarker for assessment of treatment-induced changes in this murine breast cancer model.

## Acknowledgment

This work was supported by King Abdulaziz City for Science and Technology (KACST; project number A-T-32-81).

## Disclosure

The authors declare that they do not have any conflicts of interest in this work.

## References

1. Jin S, Ye K. Targeted drug delivery for breast cancer treatment. *Recent Pat Anticancer Drug Discov*. 2013;8(2):143–153.
2. Sharma A, Jain N, Sareen R. Nanocarriers for diagnosis and targeting of breast cancer. *Biomed Res Int*. 2013;2013:960821.
3. Thakor AS, Gambhir SS. Nanooncology: the future of cancer diagnosis and therapy. *CA Cancer J Clin*. 2013;63(6):395–418.
4. Yang Z, Kang SG, Zhou R. Nanomedicine: de novo design of nanodrugs. *Nanoscale*. 2014;6(2):663–677.
5. Giles J. Top five in physics. *Nature*. 2006;441(7091):265.
6. Gong H, Peng R, Liu Z. Carbon nanotubes for biomedical imaging: the recent advances. *Adv Drug Deliv Rev*. 2013;65(15):1951–1963.
7. Vardharajula S, Ali SZ, Tiwari PM, et al. Functionalized carbon nanotubes: biomedical applications. *Int J Nanomedicine*. 2012;7:5361–5374.
8. Madani SY, Naderi N, Dissanayake O, Tan A, Seifalian AM. A new era of cancer treatment: carbon nanotubes as drug delivery tools. *Int J Nanomedicine*. 2011;6:2963–2979.
9. Kostarelos K, Bianco A, Prato M. Promises, facts and challenges for carbon nanotubes in imaging and therapeutics. *Nat Nanotechnol*. 2009;4(10):627–633.
10. Iyer AK, Khaled G, Fang J, Maeda H. Exploiting the enhanced permeability and retention effect for tumor targeting. *Drug Discov Today*. 2006;11(17–18):812–818.
11. Kostarelos K, Lacerda L, Pastorin G, et al. Cellular uptake of functionalized carbon nanotubes is independent of functional group and cell type. *Nat Nanotechnol*. 2007;2(2):108–113.
12. Lacerda L, Russier J, Pastorin G, et al. Translocation mechanisms of chemically functionalised carbon nanotubes across plasma membranes. *Biomaterials*. 2012;33(11):3334–3343.
13. Liu Z, Tabakman SM, Chen Z, Dai H. Preparation of carbon nanotube bioconjugates for biomedical applications. *Nat Protoc*. 2009;4(9):1372–1382.
14. Tacar O, Sriamornsak P, Dass CR. Doxorubicin: an update on anticancer molecular action, toxicity and novel drug delivery systems. *J Pharm Pharmacol*. 2013;65(2):157–170.
15. Al Faraj A, Sultana Shaik A, Al Sayed B. Preferential magnetic targeting of carbon nanotubes to cancer sites: noninvasive tracking using MRI in a murine breast cancer model. *Nanomedicine*. In press 2014.
16. Liu Z, Tabakman S, Welsher K, Dai H. Carbon nanotubes in biology and medicine: in vitro and in vivo detection, imaging and drug delivery. *Nano Res*. 2009;2(2):85–120.
17. Whisenant JG, Ayers GD, Loveless ME, Barnes SL, Colvin DC, Yankeelov TE. Assessing reproducibility of diffusion-weighted magnetic resonance imaging studies in a murine model of HER2+ breast cancer. *Magn Reson Imaging*. 2014;32(3):245–249.
18. Gu YJ, Cheng J, Jin J, Cheng SH, Wong WT. Development and evaluation of pH-responsive single-walled carbon nanotube-doxorubicin complexes in cancer cells. *Int J Nanomedicine*. 2011;6:2889–2898.
19. Al Faraj A, Shaik AS, Afzal S, Al Sayed B, Halwani R. MR imaging and targeting of a specific alveolar macrophage subpopulation in LPS-induced COPD animal model using antibody-conjugated magnetic nanoparticles. *Int J Nanomedicine*. 2014;9:1491–1503.
20. Yang S, Zhang JJ, Huang XY. Mouse models for tumor metastasis. *Methods Mol Biol*. 2012;928:221–228.
21. Liu Z, Fan AC, Rakhra K, et al. Supramolecular stacking of doxorubicin on carbon nanotubes for in vivo cancer therapy. *Angew Chem Int Ed Engl*. 2009;48(41):7668–7672.
22. Cai D, Mataraza JM, Qin ZH, et al. Highly efficient molecular delivery into mammalian cells using carbon nanotube spearing. *Nat Methods*. 2005;2(6):449–454.
23. Klumpp C, Kostarelos K, Prato M, Bianco A. Functionalized carbon nanotubes as emerging nanovectors for the delivery of therapeutics. *Biochim Biophys Acta*. 2006;1758(3):404–412.
24. Elhissi AM, Ahmed W, Hassan IU, Dhanak VR, D'Emanuele A. Carbon nanotubes in cancer therapy and drug delivery. *J Drug Delivery*. 2012;2012:837327.
25. Kim JB, Urban K, Cochran E, et al. Non-invasive detection of a small number of bioluminescent cancer cells in vivo. *PLoS One*. 2010;5(2):e9364.